doi:10.36487/ACG_repo/2435_D-11
9th International Conference and Exhibition on Mass Mining, Kiruna Sweden 17-19 September 2024

Back-analysis of caving propagation using numerical models in Esmeralda Sur mine's Block 1, El Teniente

R. Vidal[a], J.A. Vallejos[a], D. Cuello[b] and C. Cifuentes[c]
[a]Universidad de Chile
[b]Geomecánica Minería y Tecnología (GMT)
[c]CODELCO, Chile

ABSTRACT

Between early 2011 and 2012, two virgin caves (Esmeralda Sur's Block 1 and Block 2) commenced operations within El Teniente mine. These blocks were situated in a competent rock mass known as the mafic complex from El Teniente mine (CMET) and achieved an extraction rate of 25,000 tonnes per day (tpd). The stress conditions in this zone were significantly influenced by the proximity to the old Esmeralda's cave. Both Blocks implemented hydraulic fracturing.

Drawing upon data collected from the Esmeralda Sur mine, a continuous numerical model was developed using FLAC3D software and employed the IMASS constitutive model. The primary objective of this study was to calibrate the cave initiation, propagation, and breakthrough processes.

In conclusion, this study presents recommendations and techniques for continuous caving modelling using numerical tools.

1 INTRODUCTION

The Esmeralda sector, belonging to the El Teniente mine, CODELCO, Chile, initiated its caving process in 1996. However, by 2004, following a series of collapses, it had incurred a loss of production area of 26,000 [m^2]. Subsequently, between 2009 and 2010, a massive collapse occurred, affecting a total production area of 30,605 [m^2] ahead of the extraction front, thereby the extraction was inviable in the sector (GMT, 2018).

Due to the collapse in the old sector between 2011 and 2012, the extraction of two new blocks (Block 1 and Block 2) began in an area known as Esmeralda Sur, to continue extracting ore from the adjacent abandoned sector. The caving of both blocks commenced in a virgin competent rock mass known as mafic complex from El Teniente mine (CMET) and achieved an extraction rate of 25,000 tonnes per day [tpd]

The scope of this study is to realize a back-analysis of the cave initiation, propagation and breakthrough to the upper level extracted known as Teniente 4 (Ten4) of Block 1 (See Figure 1) using the caving propagation algorithm proposed by (Pierce et al., 2006) using the software FLAC3D.

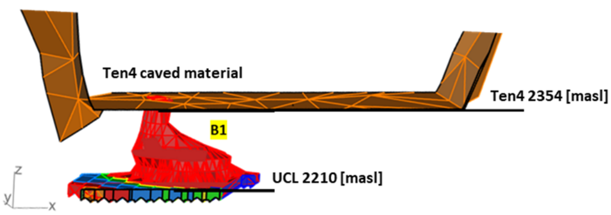

Figure 1 Estimated cave-back of Block 1 at breakthrough to Ten4 level.

2 MODELING APPROACH

The numerical model developed in this work uses the Itasca Constitutive Model for Advanced Strain Softening (IMASS) which uses Hoek & Brown criterion (Hoek et al., 2002) described by Equation (1).

$$\sigma_1 = \sigma_3 + \sigma_{ci}\left(m_b \cdot \frac{\sigma_3}{\sigma_{ci}} + s\right)^a \quad (1)$$

With the respective rock mass properties of Young modulus E_{rm} [GPa], poisson ratio and Hoek & Brown parameters a,s and m_b as function of Geological Strength Index (GSI) as shown in the following Equations.

$$E_{rm} = E_i\left(0.02 + \frac{1}{1+\exp((60-GSI)/11)}\right) \quad (2)$$

$$\upsilon = 0.032 - 0.0015 \cdot GSI \quad (3)$$

$$m_b = m_i \exp\left(\frac{GSI-100}{28}\right) \quad (4)$$

$$s = exp\left(\frac{GSI-100}{9}\right) \quad (5)$$

$$a = \frac{1}{2} + \frac{1}{6}\left(exp\left(\frac{-GSI}{15}\right) - exp\left(-\frac{20}{3}\right)\right) \quad (6)$$

The IMASS constitutive model used in this study allows to represent the degradation of Rock Mass properties induced by caving mining. Figure 2 shows the transition between envelopes as function of plastic deformation and volumetric strain. The first transition between Peak strength envelope and Post-peak envelope are expressed by plastic deformation and the Rock mass resistance are reduced until reaches the critical strain ε_{crit} which is expressed as function of GSI and zone size (Lorig & Pierce 2000) (see Equation (7)).

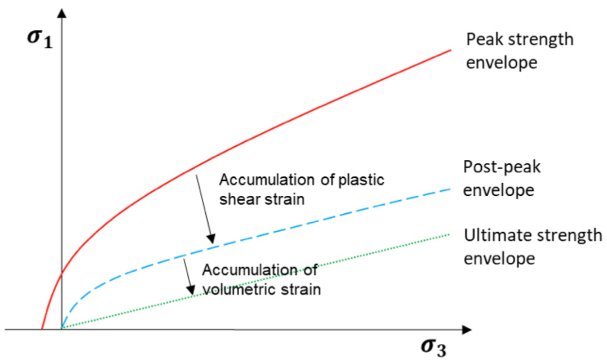

Figure 2 Yield surfaces in IMASS constitutive model (Ghazvinian et al., 2020).

$$\varepsilon_{crit} = \frac{(12.5 - 0.125 \cdot GSI)}{(100 \cdot zone\ size)} \quad (7)$$

Once the Post-peak envelope is reached, the elastic properties and density commence to be reduced as function of the volumetric strain (VSI), this process is known as bulking and is the transition between fractured rock mass to completely caved rock mass as shown in the

Figure 3. The hoek – brown properties for Post-peak envelope and residual are presented in the Table 1.

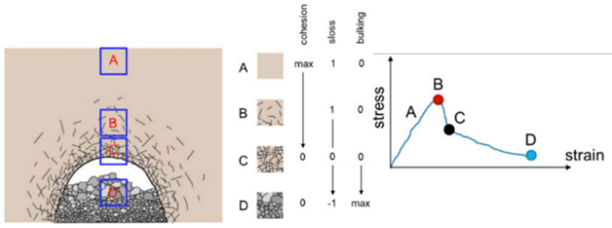

Figure 3. Schematic representation for various degrees of damage in a rock mass (Ghazvinian et al., 2020).

Table 1 Hoek - Brown constants for Post - Peak and residual envelopes

Hoek – Brown Parameter	Post – Peak	Residual
a	0.6	0.85
s	0	0
m_b	1.98	1.98

The caving algorithm used in this work simulates the production draw based on small downward-oriented velocities in the back of the undercut. According to Pierce et al. (2006) this scheme allows to control the amount of material being removed from an area. The steps of this algorithm are described in the Figure 4.

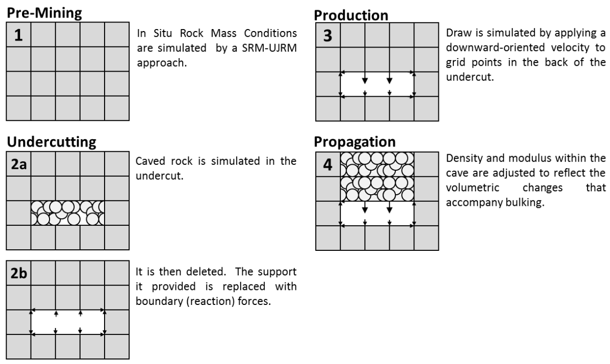

Figure 4 Simulation of production draw from large-scale, three-dimensional strain-softening continuum models based on velocities (Sainsbury 2012).

The material extracted from the undercut could be calculated as incremental expression given by the following equation, where m corresponds to the extracted mass, V [m/step] the downward-oriented nodal velocity, t the time step, A [m^2] the influence area of each extraction active point and ρ [kg/m^3] the density.

$$m = V \cdot t \cdot A \cdot \rho \quad (2)$$

3 MODEL CONSTRUCTION

The numerical model was developed by tetrahedral elements considering the geometry of old caved material as explicit volume, illustrated by Figure 5 and explicit geological structures or interfaces (See Figure 6).

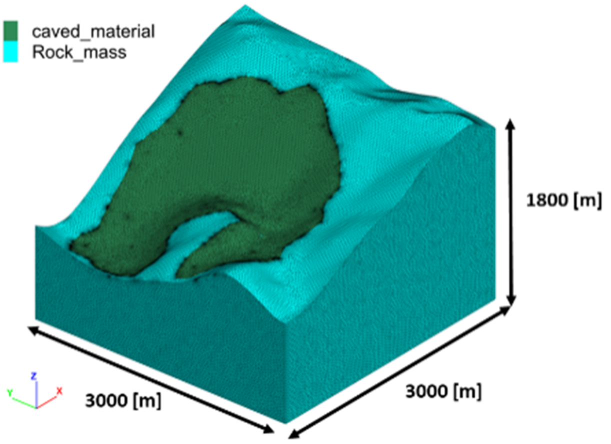

Figure 5 Dimensions of numerical model.

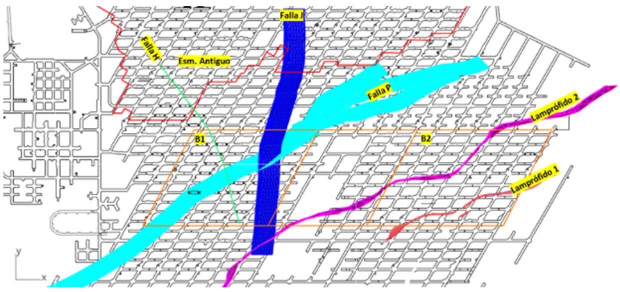

Figure 6 Top view of Esmeralda Sur structural model.

4 BACK ANALYSIS OF CAVING PROPAGATION IN BLOCK 1

4.1 Geotechnical properties and assumptions

The geotechnical properties used in the Block 1 model are the same that were proposed by Vallejos et al. (2014). The properties of the structures used in the model with residual cohesion of 0 [kPa] are presented in the Table 3. These properties are based on the geological study realized by Millán & Brzovic (2014).

Table 2 Rock mass properties of the model (Vallejos et al. 2014)

Rock Unit	GSI	m_i	σ_{ci} [MPa]	E_{rm} [GPa]
Diorite porphyry	62	11.3	140	9.2
CMET Hw	65	11.0	121	15.2

Table 3 Interface properties for faults in Macroblock S02

Property	K_n [GPa/m]	K_s [GPa/m]	C [kPa]	Φ [°]
Value	1.87	0.23	120	25

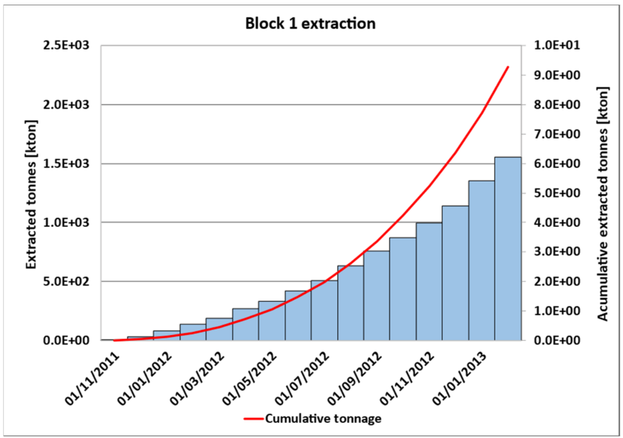

Figure 7 Draw schedule for Block 1.

The stresses of the models were initialized by the stress tensor presented by Equation (8) as function of the depth (z) in meters.

$$\begin{aligned} \sigma_{zz} &= 0.027 \cdot z\ [MPa] \\ \sigma_{ew} &= \sigma_{zz} \cdot 1.2\ [MPa] \\ \sigma_{ns} &= \sigma_{zz} \cdot 1.7\ [MPa] \\ \sigma_{ew-ns} &= 0.0\ [MPa] \\ \sigma_{ns-z} &= 0.0\ [MPa] \\ \sigma_{ew-z} &= 0.0\ [MPa] \end{aligned} \quad (8)$$

The pre-mining stress at UCL level in Block 1 are summarized in the Table 4.

Table 4 Block 1 pre-mining stress at UCL (2210 [masl])

Component	Magnitude [MPa]	Trend	Plunge
σ_1	37	186.5°	8.3°
σ_2	32	262.3°	7.2°
σ_3	19	52.5°	81.5°

4.2 Caving response on Block 1

The production schedule during the period of analysis used to simulate the caving initiation, propagation, and breakthrough to Ten4 level are presented in Figure 7.

To calibrate the caving response of Block 1 estimated cave-backs that are summarized in Figure 8 was used.

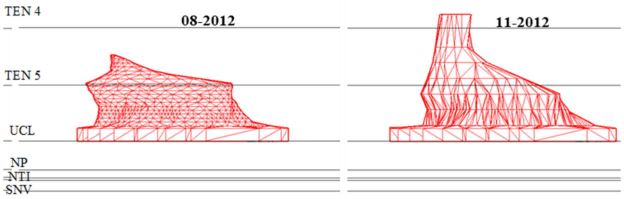

Figure 8 Front view of estimated cave-backs in Block 1 (GMT, 2018).

5 MODEL RESULTS

The simulated cave shape was interpreted using displacement criteria with vertical displacement lower than -1 meters and available seismicity data. To analyze the results two dates are presented August 2012 and October 2012 in this work. Figure 9 shows the section A – A' which is used to show the cavity growth in detail.

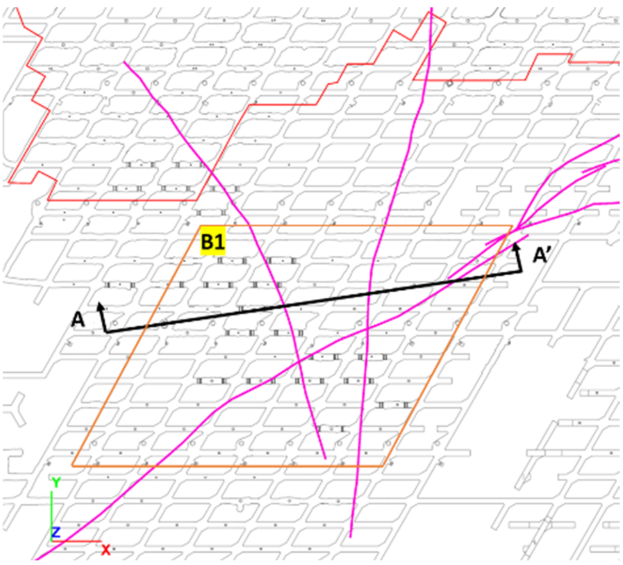

Figure 9. Top view of section A - A'.

In August 2012, Figure 10 shows an isometric view of the simulated cavity with seismic events as scalars. The results indicates that the cave growth was delimited by geological structures and the seismic events are concentrated at the cave-back. This behavior could be seen in more detail in the section view illustrated by the Figure 11.

Respect to the cave breakthrough to Ten4 level, The connection is also influenced by faults as shown in Figure 12 and Figure 13 and the seismicity was consistent with the geometry of the simulated cave-back.

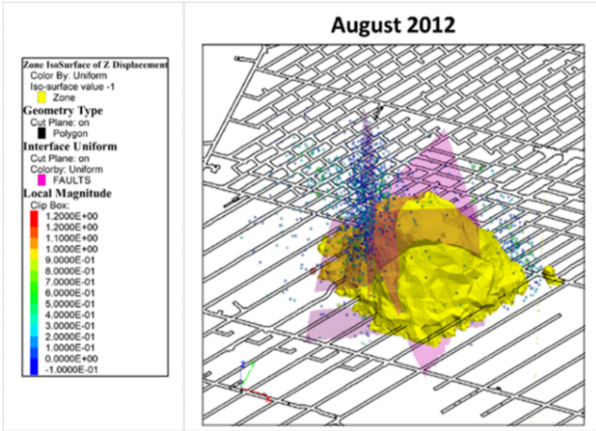

Figure 10. Isometric view of simulated cavity and seismicity registered in August 2012.

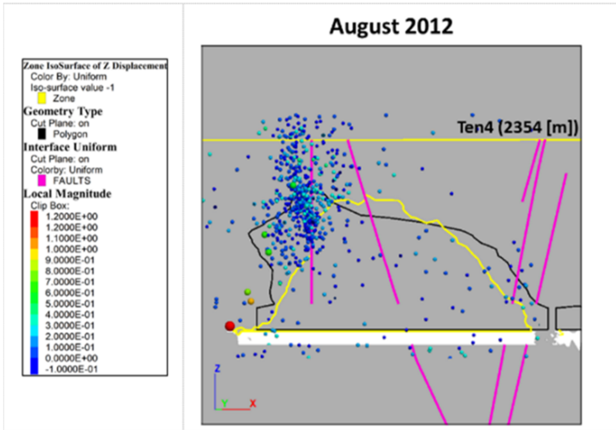

Figure 11. Section A - A' of simulated cavity and seismicity registered in August 2012.

6 CONCLUSIONS

The cave propagation is mainly and breakthrough to the upper are controlled by the geological structures and it is consistent with the seismic events and estimated geometry of cave-backs.

Compared to the previous study of this zone realized by Itasca in 2017 using 3DEC software with explicit structures defined as joints, the results of this model with interfaces are similar, remarking that the FLAC3D software is much faster than 3DEC in continuous caving modeling. Therefore, is recommended simulate the caving propagation with FLAC3D.

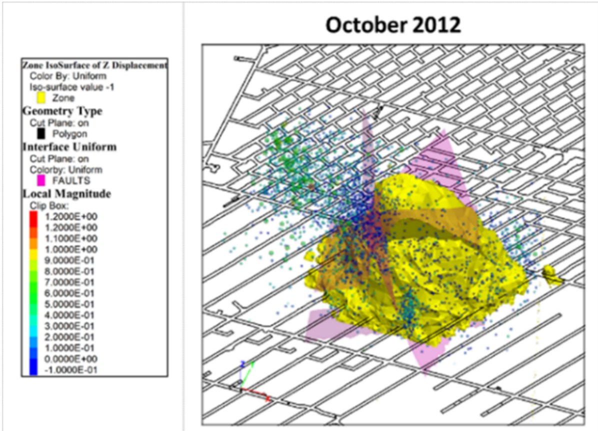

Figure 12. Isometric view of simulated cavity and seismicity registered in October 2012.

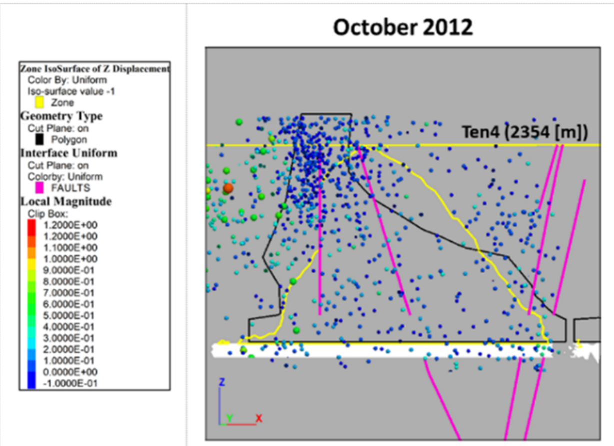

Figure 13 Section A - A' of simulated cavity and seismicity registered in October 2012.

The impact of preconditioning on Block 1 remains under study and will be published at another instance.

ACKNOWLEDGEMENT

The first two authors gratefully acknowledge the support from basal project FB-0809 of Advanced Mining Technology Center (AMTC) and by the CONICYT/PIA Project AFB180004/AFB220002/AFB230001. The FLAC3D software license provided by Itasca Chile Spa for the study is also gratefully acknowledge.

REFERENCES

Álvarez, C., Gómez, P., Orrego, C. & López, S. (2020). Calibration of structurally controlled caving propagation using 3DEC. The Esmeralda Block 1 case study. In MassMin 2020: Proceedings of the Eighth International Conference & Exhibition on Mass Mining (pp. 418-427). University of Chile.Millán, J & Brzovic, A. (2014). "Review of Physical-Mechanical Properties for intact rock and El Teniente faults", Internal Report. GRMD-SGL-INF-081-2014, Rancagua, Chile, in Spanish.

Duplancic, P. & Brady, B. H. (1999). Characterisation of caving mechanisms by analysis of seismicity and rock stress. In G. Vouille & P. Berest (Eds.), Characterisation of caving mechanisms by analysis of seismicity and rock stress. (Vol. 2, pp. 1049-1053). Rotterdam, Netherlands: CRC Press/Balkema.

Ghazvinian, E., Garza-Cruz, T., Bouzeran, L., Fuenzalida, M., Cheng, Z., Cancino, C. & Pierce, M. (2020). Theory and Implementation of the Itasca Constitutive Model for Advanced Strain Softening (IMASS). MassMin 2020, Proceedings of the Eighth International Conference & Exhibition on Mass Mining.

GMT (2018). Back-analysis of caving initiation and propagation of Block 1 and 2 on Esmeralda Mine. Internal report. ICAV-B1B2-ESM-DET-01, in Spanish.

Lorig, L. & Pierce, M. (2000). Methodology and Guidelines for Numerical Modelling of Undercut and Extraction-Level Behaviour in Caving Mines. Itasca Consulting Group, Inc., Report to the International Caving Study, ICG00-099-6-15F, October 2000.

Pierce, M., Cundall, P., Mas Ivars, D., Darcel, C., Young, R.P., Reyes-Montes, J. & Pettitt, W. (2006). Six Monthly Technical Report, Caving Mechanics, Sub-Project No. 4.2: Research and Methodology Improvement, and Sub-Project 4.3, Case Study Application", Itasca Consulting Group Inc, Report to Mass Mining Technology Project, 2004-2007, ICG06-2292-1-Tasks 2-3-14, March.

Sainsbury, B.-A. (2012). A Model for Cave Propagation and Subsidence Assessment in Jointed Rock Masses. PhD thesis, University of New South Wales